ELSEVIER

Journal of Fluids and Structures 20 (2005) 71–80

JOURNAL OF FLUIDS AND STRUCTURES

www.elsevier.nl/locate/jnlabr/yjfls

An experimental study on feedback control of rotating disk flutter

X.Y. Huang*, M.E. Hoque, X. Wang

Center for Mechanics of Micro-Systems, School of Mechanical and Production Engineering, Nanyang Technological University, Nanyang Avenue, Singapore 639798, Singapore

Received 15 November 2002; accepted 2 October 2004
Available online 2 January 2005

Abstract

An experimental study is presented in this paper to demonstrate the feedback control of rotating disk flutter. In the experiment, steel disks were rotated between two solid plates and the disk flutter was detected by a laser-Doppler vibrometer. The disk vibration signals were then processed to drive a speaker mounted on one of the supporting plates. The air pressure generated by the speaker was applied to the disks, through a hole in the plate, acting as the control force. The disk mode frequencies, critical speed and flutter speeds were measured for two disks with different sizes, and the results were compared with predicted values. It is shown that the feedback control can effectively suppress the flutter on a large disk (135 mm diameter) rotating up to 11 000 rpm and on a small disk (100 mm diameter) rotating up to 15 000 rpm. Further improvement of the control technique is also discussed.

1. Introduction

Rotating disk flutter is an aeroelastic instability induced by the coupling of the disk vibration to the air around the disk. The flutter may occur at high rotation speed and the disk will then vibrate with large amplitude. The stability of rotating disks has recently become an important research topic, owing to its applications related to the high-capacity and high-performance data storage devices, such as hard disk drives for computers. The disk flutter has been a concern to the data storage industries in order to develop high-speed hard disk drives, and intensive research has been conducted, mainly focused on the modelling and suppression of the rotating disk flutter in hard disk drives.

D'Angelo and Mote (1993) conducted an experiment on thin disks in an enclosure with different air densities. They reported that the critical flutter speed would increase with a decrease of the air density and confirmed that the flutter was induced by the aerodynamic coupling of the air to the rotating disk. Renshaw et al. (1994) presented an analytical study of the flutter of a rotating disk by taking into account the air coupling and examining the eigenvalues of the whole disk system. Other analytical studies (Hosaka and Crandall, 1992; Yasuda et al., 1992; Chonan et al., 1992; Huang and Mote, 1995; Renshaw, 1998) were conducted on rotating disks close to rigid surfaces, which are associated with floppy disks used in personal computers. The aerodynamic coupling between the rotating disks and the surrounding air is crucial to the onset of the flutter. Kim et al. (2000) and Hansen et al. (2001) examined different models of the aerodynamic loading on rotating disks.

*Corresponding author. Tel.: +65 790 4448.
E-mail address: mxhuang@ntu.edu.sg (X.Y. Huang).

0889-9746/$ - see front matter
doi:10.1016/j.jfluidstructs.2004.10.001

Several methods have been developed in the disk drive industry to reduce or suppress the disk flutter. Heo et al. (2000) studied experimentally the effect of the base castings of the hard disk drives on disk flutter, and reported that the disk flutter could be reduced up to 50% by smoothening the shroud contour and reducing the shroud opening. Imai et al. (1997) suggested a centrifugal airflow system in a 3.5-in hard disk drive. The centrifugal airflow system emitted air to the gaps between disks through holes in the disk spacer. The disk flutter amplitudes were reduced 40–60% with this technique. A squeeze air film between a plate and a rotating disk was found effective in suppressing the disk flutter, as reported by Bittner and Shen (1999), Ono and Maeda (2000) and Deeyiengyang and Ono (2001). All these methods are passive control techniques, which either modified the configuration of the disk drive castings and aerodynamics of the disks, or increased the dynamic damping of the disk.

Huang et al. (2004) proposed an active control method to suppress the rotating disk flutter, in which the disk vibration signals were detected and processed to generate pressure perturbations inside the disk enclosure in such way that the original coupling would be altered and the disk flutter was therefore suppressed. This was shown theoretically by a dynamic stability study on a disk-air-enclosure system. In the present paper, an experiment was conducted on a disk rotating between fixed plates to demonstrate that rotating disk flutter can be controlled by this active method. The theoretical model was modified to take into account the difference between the two plates and the enclosure. The comparison between the experimental results and predicted values was carried out on the disk mode frequencies, critical speeds and flutter speeds.

2. Experimental set-up

The experimental set-up is illustrated in Fig. 1. It consists of a disk with a driving system, a disk vibration measurement and analysis system, and a feedback control system. Two steel disks were used in the experiment. One (disk-1) had thickness of 0.29 mm and diameter of 130 mm, the other (disk-2) had thickness of 0.25 mm and diameter of 100 mm. Both disks had a 25 mm diameter hole at their centers for fixing onto the driving motor, and were clamped by a clamping collar and a supporting collar of diameter 31 mm. The disk and motor assembly is shown in Fig. 2. The motor was a standard motor used in hard disk drives, and was driven by a motor-control board together with a square-wave generator. The motor rotation speed can be varied from a few hundred rpm up to 15 000 rpm, and monitored by a digital counter. The disk and the motor were held between two plates of 160 mm in height and 240 mm in width. The gap between the plates was 14 mm, and the front plate was 3 mm away from the disk surface. The front plate was made of 5 mm Perspex, so that a laser beam can go in/out for the disk vibration measurement. The disk vibrations were measured by a laser-Doppler vibrometer (Ometron VPI Sensor) and the output signals were analyzed by a HP digital signal analyzer to obtain the spectra and the waterfall plots of the disk vibrations. Apart from the disk vibrations, the output signals from the laser sensor also contained components associated with the disk rotation. The feedback control system consisted of a frequency filter, a phase shifter, an amplifier and a speaker. The frequency filter was a band-pass

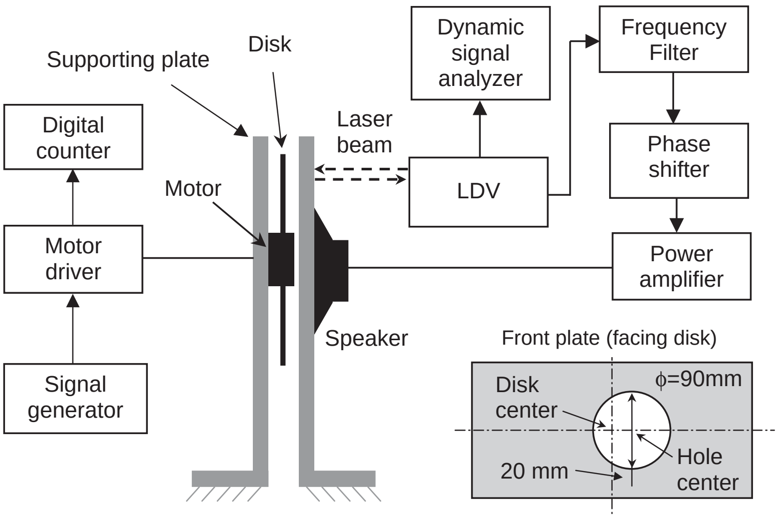

Fig. 1. A schematic illustration of experimental set-up for the disk and the feedback control system.

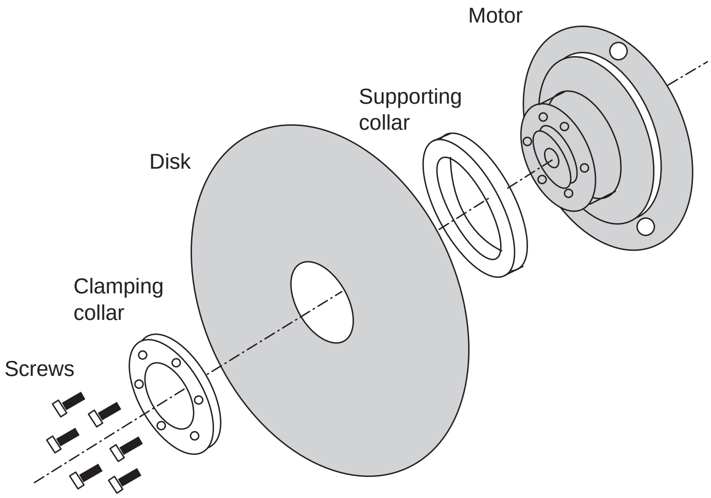

Fig. 2. The disk and the motor assembly.

filter which had bandwidth 10 Hz and the center frequency set according to the disk flutter frequency to be controlled. The reduction was more than 20 dB for signals having frequency outside the frequency band. The speaker (4 in and 30 W) was mounted on the front plate and the acoustic pressure generated by the speaker was applied to the disk through a 90 mm diameter hole on the front plate, as shown in Fig. 1. The phase shifter was used to change the phase of the feedback signals from the input disk vibrations, before being amplified to drive the speaker.

3. Modification of the theoretical model

Theoretical calculations were carried out on disk mode frequencies, critical speed and flutter speeds. The theoretical model used in the present study was basically similar to the one for a disk rotating in an enclosure (Huang et al., 2004), but was modified to take into account the difference in geometry configurations and disk properties. The modifications were limited to the following two parts. Firstly, for the disk rotated inside an enclosure, the boundary condition for the acoustic velocity potential ϕ_a at the sidewall of the enclosure was

$$\left.\frac{\partial \phi_a}{\partial r}\right|_{r=r_e} = 0. \tag{1}$$

Since the disk in the present experiment was rotated between two plates without the sidewall, the boundary condition for the acoustic velocity potential ϕ_a was changed in this case to be

$$\phi_a|_{r=r_e} = 0. \tag{2}$$

Secondly, the speed ratio Ω_d/Ω, which is a parameter in the empirical aerodynamic loading term used in the theoretical model, was set to be 0.8 in the previous study for the enclosure. In the present study, we found that by setting $\Omega_d/\Omega = 0.85$ the predicted disk flutter speeds agreed well with the experimental values for both disk-1 and disk-2. The variation of Ω_d/Ω from 0.8 to 0.85 was probably due to the configuration difference. The details related to the modelling can be found in the paper by Huang et al. (2004).

The control actuator in the model study, for both enclosure and two plates, was a flat disk actuator being part of the enclosure top cover (or the front plate), while the actuator in the experiment was an air column generated by the speaker, which was an approximation to the model study. This part, of course, can be improved by using piezo actuators. In our experiment, the hole in the front plate for the speaker was off-centered to the disk center, as shown in Fig. 1, so that the pressure generated over the disk was not uniform. This is to produce the actuator distribution function, $A(r, \theta)$, used in the theoretical model (Huang et al., 2004).

4. Results and discussion

4.1. Disk vibration modes and critical speeds

The experiments were started with the measurement of the modal frequencies for the disks at stationary conditions, followed by the disk critical speed and flutter speed measurement, and finally the feedback control. The disk modal frequencies were measured by the standard hammer impact method, and a typical result is shown in Fig. 3 for disk-2. Disk modes are denoted by (m, n), where m is the number of circumferential nodes and n is the number of radial nodes. The measured modal frequencies are tabulated in Table 1, compared with the theoretically predicted values. The frequencies of modes (0, 0) and (0, 1) are very close, and most of time the hammer impact test produced essentially one peak for these two modes, as shown in Fig. 3. The discrepancy between the measured values and prediction was large for these two modes, which was also reported by others [e.g., D'Angelo and Mote (1993)] probably due to imperfection of the clamping at the center of the disks and nonuniformity of the disk thickness. The agreement between the measured results and the predicted values is generally good for higher modes, on which the following studies on the critical speed, flutter speed and flutter control are focused.

When the disk rotates at speed Ω, these modes, except the mode (0, 0), will split into forward traveling waves (FTW) with frequency f^F_{mn} and backward traveling waves (BTW) with frequency f^B_{mn}, if they are measured from a fixed frame (Hansen et al., 2001). In the theoretical calculation, the split of the mode frequency corresponds to a pair of eigenvalues, λ^F_{mn} and λ^B_{mn}. The real parts of λ^F_{mn} and λ^B_{mn} are modal frequencies, the imaginary parts of λ^F_{mn} and λ^B_{mn} are aerodynamically induced damping. The FTW and BTW mode frequencies were calculated, and the results for disk-1 are shown in Fig. 4. It can be seen that the frequencies for all FTW modes increase with rotation speed, while the frequencies for BTW modes initially decrease with rotation speed, until reaching zero at a critical speed, and then increase with the rotation speed beyond that. The critical speed differs from mode to mode. An exception is mode (0, 1)B, which has no critical speed. In order to measure the critical speeds, waterfall plots were generated for both disks. At each rotation speed (before flutter occurred), the disks were lightly tapped to excite the vibration modes and the vibration spectra were recorded.

The waterfall plot for disk-2 is presented in Fig. 5, which shows that the BTW mode frequencies are shifted with rotation speed. The calculated BTW modes frequencies varying with rotation speeds are compared with the measured results and are shown in Fig. 6(a) and (b). It is seen that the measured mode frequencies, denoted by the data-points, follow reasonably well the predicted curves denoted by the solid lines, especially for disk-1. The calculated critical speeds are compared with the values estimated from the experiment in Table 2 for modes (0, 2)B, (0, 3)B and (0, 4)B, showing that the predicted critical speeds are reasonably close to the measured values for both disks.

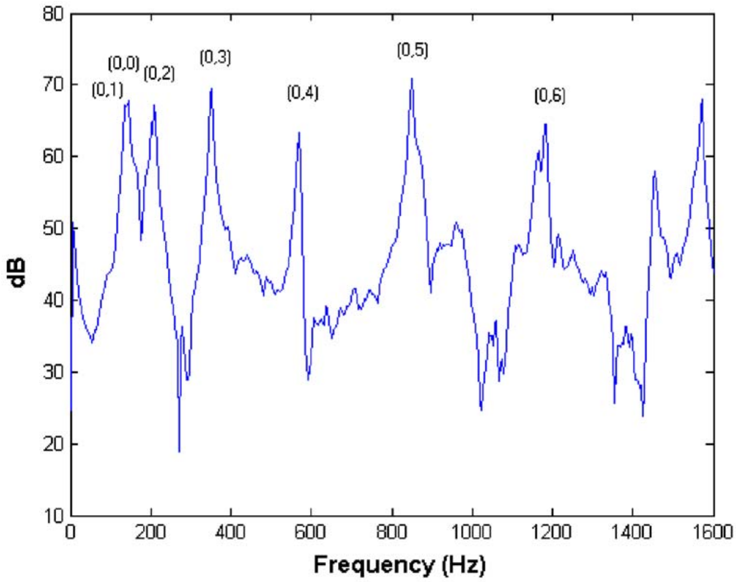

Fig. 3. A typical hammer impact test result for disk-2 (100 mm diameter).

Table 1
Mode frequencies of the stationary steel disks

Vibration mode	Modal frequencies			
	Disk-1		Disk-2	
	Predicted result	Measured result	Predicted result	Measured result
(0, 0)	87	77	167	140
(0, 1)	83	73	165	134
(0, 2)	107	108	206	204
(0, 3)	198	213	339	352
(0, 4)	339	358	560	572
(0, 5)	519	536	850	852
(0, 6)	734	754	1153	1186

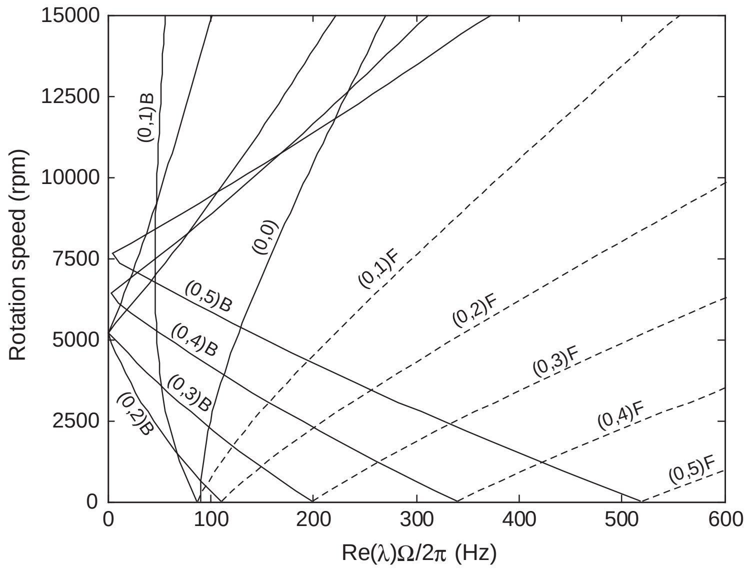

Fig. 4. Real parts of the eigenvalues from the modelling, which are the mode frequencies against the rotation speeds for disk-1 (135 mm diameter). The mode numbers (m, n) are indicated by the brackets and FTW and BTW are denoted by F and B, respectively.

4.2. Disk flutter observations

In the experiment, we observed that disk flutter occurred at a rotation speed well above the critical speed of modes (0, 2) and (0, 3). This is illustrated in Figs. 7(a) and (b) in the form of waterfall plots. In the waterfall plots, some peaks are associated with the disk rotations and their harmonics. These peak are always present as long as the disks rotate. The peaks at high rotation speed but low-frequency range are associated with strong disk vibrations and are disk flutter. Some BTW modes are also plotted on the figures by the solid lines which show that flutter occurs at the rotation speed above the critical speeds for modes (0, 2) and (0, 3). It is seen that disk flutter for both disk-1 and disk-2 is likely at mode (0, 3), which was also reported by D'Angelo and Mote (1993) and Lee et al. (2002). The flutter speeds are estimated from these plots with errors about ± 300 rpm.

In the theoretical prediction, the flutter speed was calculated based on the speed at which the imaginary part of the disk mode eigenvalue changes from positive-to-negative, as shown in Fig. 8 for disk-1, indicating that the disk became unstable. From Fig. 8, it is seen that the flutter indeed occurs first at mode (0, 3) and the flutter speed is 7300 rpm. The predicted flutter speeds for both disks agree well with the flutter speeds estimated from the waterfall plots in Fig. 7, and the comparisons are tabulated in Table 3.

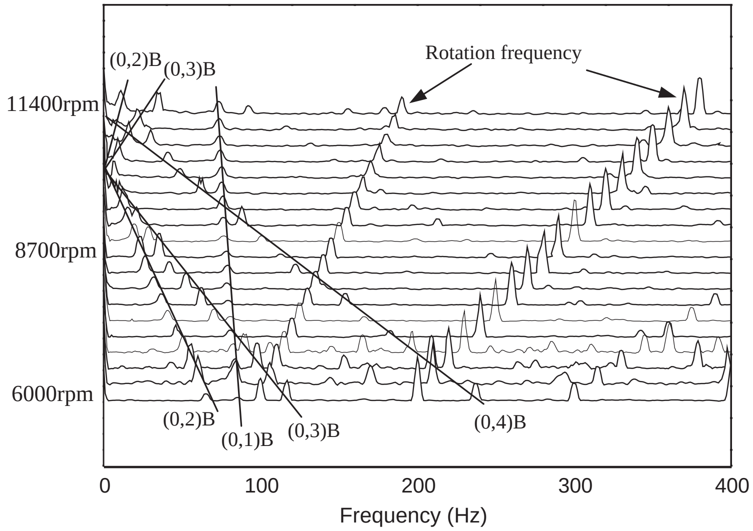

Fig. 5. Waterfall plot of disk vibration spectra at different rotation speed for disk-2.

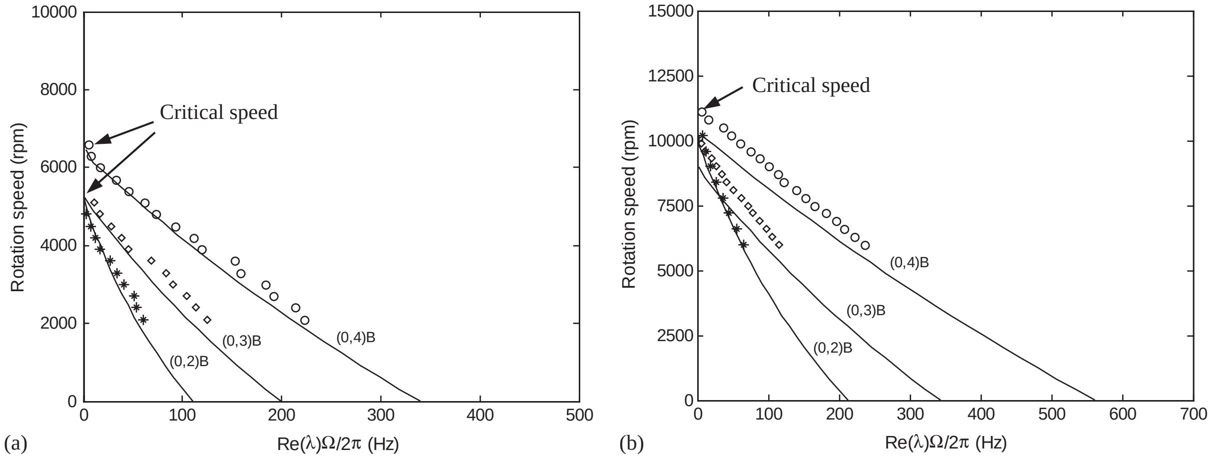

Fig. 6. Comparison of calculated modal frequencies with experimental results for (a) disk-1 and (b) disk-2. The solid lines are predicted values and the scattered points are experimental data.

Table 2
Critical speeds of BTW modes

Vibration mode	Critical speeds (rpm)			
	Disk-1		Disk-2	
	Predicted result	Measured result	Predicted result	Measured result
(0, 2)B	5200	~5400	10000	~10 200
(0, 3)B	5300	~5700	9000	~10 100
(0, 4)B	6400	~6700	10500	~11 100

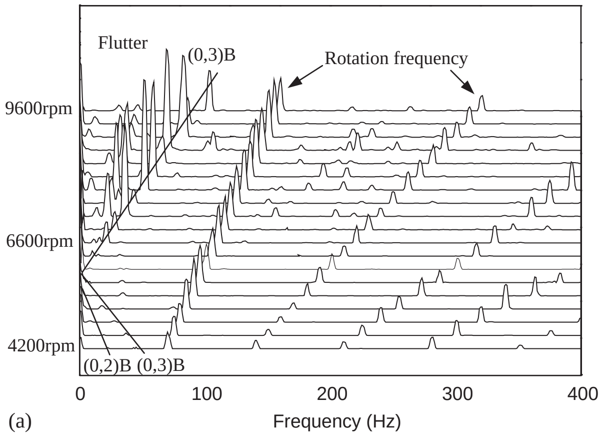

Fig. 7. Waterfall plots for (a) disk-1 and (b) disk-2 to observe the disk flutter and to estimate the flutter speeds.

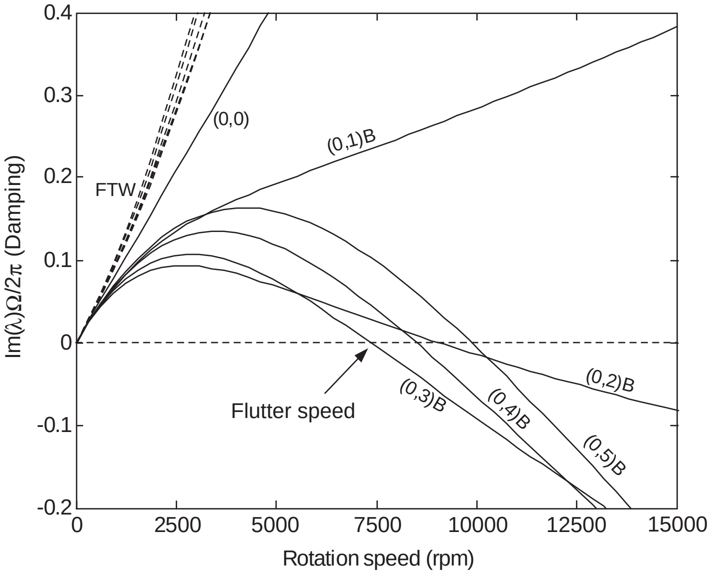

Fig. 8. Imaginary parts of the eigenvalues from the modelling, which are the damping against the rotation speeds for disk-1. The mode numbers (m, n) are indicated by the brackets.

Table 3
Flutter speed (rpm) at mode (0, 3)

Disk-1		Disk-2	
Predicted result	Measured result	Predicted result	Measured result
7300	~7200	12 200	~12 300

4.3. Feedback control of disk flutter

In the experiment on rotating disk flutter control, the disk was initially set to rotate at a speed at which the flutter peak was observed from the disk vibration spectra. The feedback loop was then closed by switching on the speaker, and the amplifier gain and the phase shifter were adjusted slowly until the flutter peak on the disk vibration spectra was reduced. The phase shifter and the gain were adjusted further until the flutter peak was reduced to a minimum. Figs. 9(a) and (b) show the control effect for disk-1 rotating at 9000 and 10 000 rpm, respectively. It is seen, by comparing the original flutter spectra (thin lines) to the controlled spectra (thick lines), that the flutter amplitudes have been suppressed almost completely.

The control effect was also simulated for the disk setup in the present experiment, and results are shown in Fig. 10 for mode (0, 3) on disk-1. The flutter control is seen to be very sensitive to the phase shift. If the control phase is reversed by 180°, from $\pi/2$ to $-\pi/2$, the flutter speed will be decreased, as indicated in Fig. 10. In other words, the flutter will be enhanced and the disk vibration will be excited in this case. This is confirmed in the experiment and the result is illustrated in Fig. 11, in which disk-1 was in the same operating condition as in Fig. 9(b) but the control phase shift was

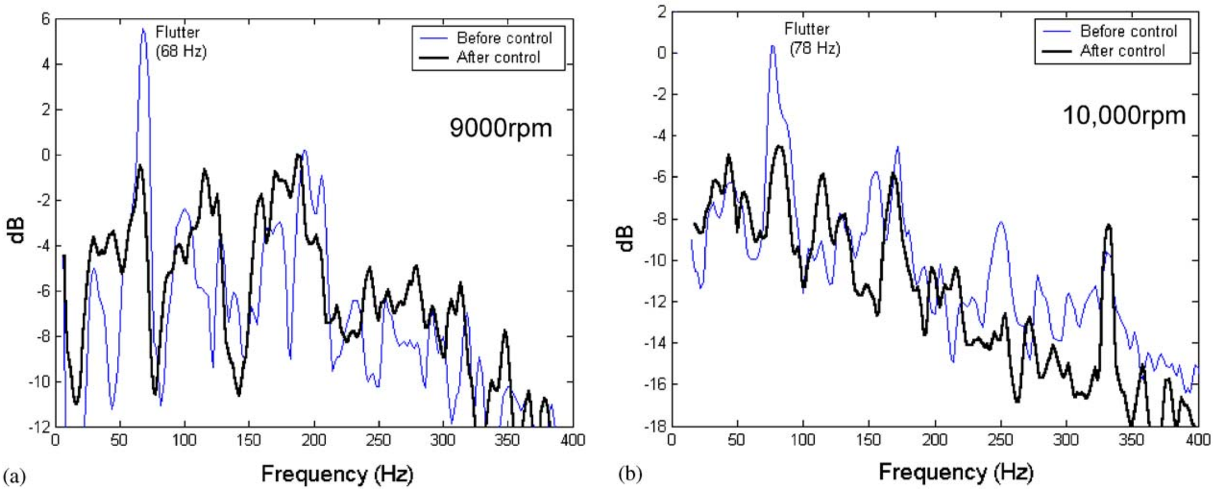

(a) (b)

Fig. 9. The disk vibration spectra showing the feedback control results for disk-1 rotated at (a) 9000 rpm, and (b) 10 000 rpm. The thin lines are the spectra without control and the thick lines are the spectra under the control.

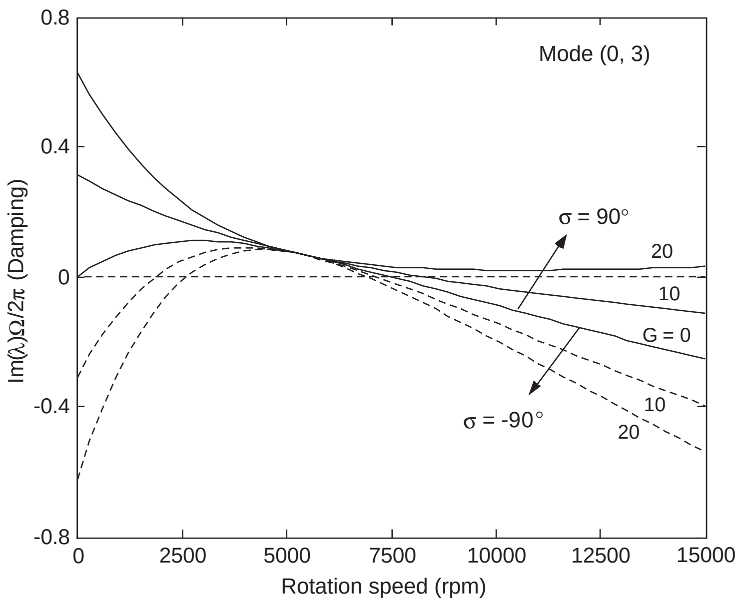

Fig. 10. Effect of the control on mode (0, 3) of disk-1. Im(λ) is associated with the aerodynamically induced damping, G is the control gain and σ is the control phase shift.

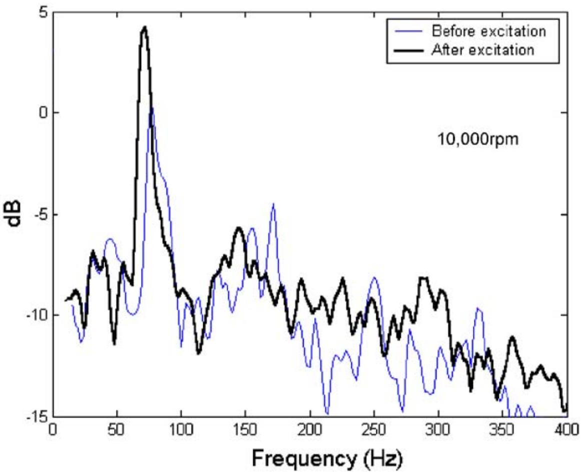

Fig. 11. The disk vibration spectra showing the disk is under excitation by reversing the phase shift from the control state for disk-1 in Fig. 5(b). The thin lines are the spectra without excitation and the thick lines are the spectra under the excitation.

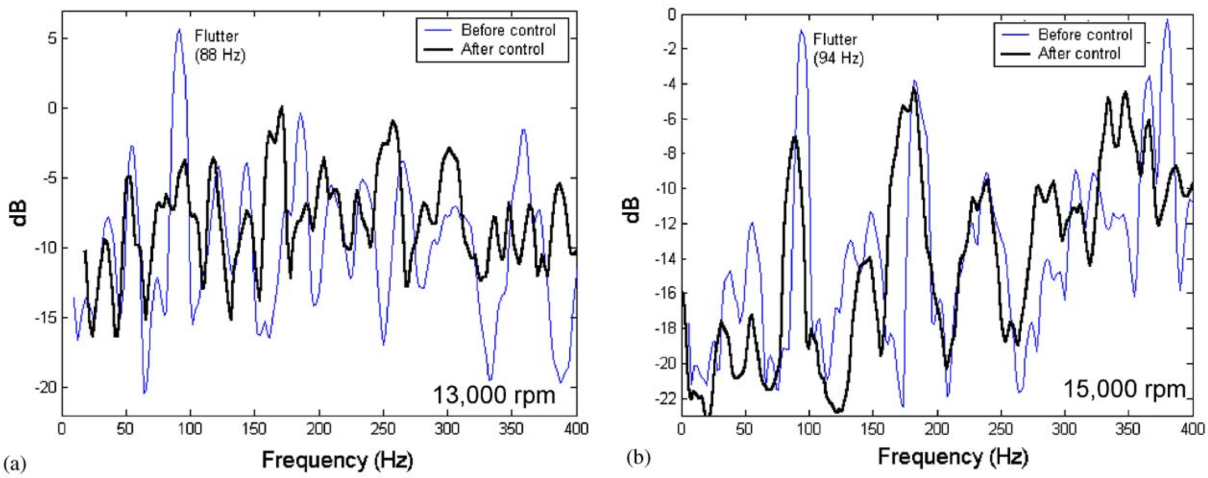

Fig. 12. The disk vibration spectra showing the feedback control results for disk-2 rotated at (a) 13 000 rpm and (b) 15 000 rpm. The thin lines are the spectra without control and the thick lines are the spectra under the control.

reversed. The control phase shift was found to be around 90°, varying from 60° to 100° in the experiment, which agreed with the predicted phase shift range for flutter control (Huang et al., 2004).

The motor used in the present experiment can only drive disk-1 up to 11 000 rpm, and for high rotation speeds the experiment was conducted on disk-2 that can rotate up to 15 000 rpm. The feedback control was seen to be still effective at 13 000 rpm, shown in Fig. 12(a), where the flutter peak has been suppressed by the control. The flutter on disk-2 at 15 000 rpm was seen to be very strong and the control results were not as good as those at lower speeds, shown in Fig. 12(b). The flutter is probably too strong at this speed to be controlled by the feedback control system.

5. Conclusions

An experiment has been conducted on feedback control of rotating disk flutter. The disks were rotated between two plates and disk vibrations were detected by a laser-Doppler vibrometer. The disk vibration signals were processed to drive a speaker which generated a control pressure on the disk to suppress the flutter. The theoretical model used for disks in an enclosure (Huang et al., 2004) was modified in the present study for the disks between two fixed plates, and the predicted disk modal frequencies, critical speeds and flutter speeds were compared with the experimental results. In the experiments, disk flutter was observed to occur at rotation speeds well above the critical speeds of modes (0, 2) and (0, 3), illustrated by the waterfall plots of the disk vibrations. The feedback control was found to be effective to suppress the flutter within the experimental speed range. The control effect was sensitive to the phase shift of the feedback signals, and the control can be changed from suppressing the flutter to exciting the flutter by reversing the phase. The experiments presented in this paper demonstrate the feasibility of using feedback control to suppress rotating disk flutter. The experiments need to be improved by having better actuating methods, such as piezo actuators, and operating at higher speeds.

Acknowledgments

The authors would like to acknowledge the financial support provided by Agency for Science, Technology & Research of Singapore and Center for Mechanics of Micro-Systems, Nanyang Technological University.

References

Bittner, H., Shen, I.Y., 1999. Taming disk/spindle vibrations through aerodynamic bearings and acoustically tuned-mass dampers. IEEE Transactions on Magnetics 35, 827–832.

Chonan, S., Jiang, Z.W., Shyu, Y.J., 1992. Stability analysis of a 2″ floppy disk drive system and the optimum design of the disk stabilizer. Journal of Vibration and Acoustics 114, 283–286.

D'Angelo, C., Mote Jr., C.D., 1993. Aerodynamically excited vibration and flutter of a thin disk rotating at supercritical speed. Journal of Sound and Vibration 168, 15–30.

Deeyiengyang, S., Ono, K., 2001. Suppression of resonance amplitude of disk vibrations by squeeze air bearing plate. IEEE Transactions on Magnetics 37, 520–825.

Kim, B.C., Raman, A., Mote Jr., C.D., 2000. Prediction of aeroelastic flutter in a hard disk drive. Journal of Sound and Vibration 238, 309–325.

Hansen, M.H., Raman, A., Mote Jr., C.D., 2001. Estimation of nonconservative aerodynamic pressure leading to flutter of spinning disks. Journal of Fluids and Structures 15, 39–57.

Heo, B., Shen, I.Y., Riley, J.J., 2000. Reducing disk flutter by improving aerodynamic design of base castings. IEEE Transactions on Magnetics 36, 2222–2224.

Hosaka, H., Crandall, S., 1992. Self-excited vibrations of a flexible disk rotating on an air film above a flat surface. Acta Mechanica 3, 115–127.

Huang, F., Mote Jr., C.D., 1995. On the instability mechanism of a disk rotating close to a rigid surface. Journal of Applied Mechanics 62, 764–771.

Huang, X.Y., Wang, X.Z., Yap, F.F., 2004. Feedback control of rotating disk flutter in an enclosure. Journal of Fluids and Structures 19, 917–932.

Imai, S., Mori, T., Okazaki, T., 1997. Flutter reduction by centrifugal airflow for high-rotation-speed disks. International Proceedings on Micromechatronics for Information and Precision Equipment, Tokyo, July 20–23.

Lee, S.Y., Kim, J.D., Kim, S., 2002. Critical and flutter speeds of optical disks. Microsystem Technologies 8, 206–211.

Ono, K., Maeda, E., 2000. Suppression of disk flutter by a squeeze air-bearing plate. Journal of Information Storage and Processing Systems 2, 1–2.

Renshaw, A.A., 1998. Critical speeds for floppy disks. Journal of Applied Mechanics 65, 116–120.

Renshaw, A.A., D'Angelo, C., Mote Jr., C.D., 1994. Aerodynamically excited vibration of a rotating disk. Journal of Sound and Vibration 177, 577–590.

Yasuda, K., Torii, T., Shimizu, T., 1992. Self-excited oscillations of a circular disk rotating in air. JSME International Journal 35, 347–352.